Molecular Dynamics of Microbial Lipases as Determined from Their Intrinsic Tryptophan Fluorescence

M. Graupner,* L. Haalck,# F. Spener,# H. Lindner,§ O. Glatter,§ F. Paltauf,* and A. Hermetter*
*Department of Biochemistry, Technische Universität Graz, A-8010 Graz, Austria; #Department of Biochemistry, University of Münster, D-48149 Münster, Germany; and §Department of Physical Chemistry, University of Graz, A-8010 Graz, Austria

ABSTRACT We have studied the intrinsic tryptophan fluorescence of the lipases from *Chromobacterium viscosum* (CVL), *Pseudomonas species* (PSL), and *Rhizopus oryzae* (ROL) in aqueous buffer, zwitterionic detergent micelles, and isopropanol-water mixtures. It was the purpose of this study to obtain information about biophysical properties of the respective enzymes under conditions that modulate enzyme activities and stereoselectivities to a significant extent. According to their decay-associated emission spectra, CVL tryptophans are located in the hydrophobic interior of the protein. In contrast, the PSL and ROL tryptophans are probably confined to the core and the surface of the lipase. From the tryptophan lifetime distributions it can be concluded that the conformation of CVL is not much affected by detergent or organic solvent (isopropanol). Accordingly, CVL is enzymatically active in these systems and most active in the presence of isopropanol. In contrast, ROL and PSL show high conformational mobility, depending on the solvent, because their lifetime distributions are very different in the presence and absence of detergent or isopropanol. Time-resolved anisotropy studies provided evidence that the lipases exhibit very high internal molecular flexibility. This peculiar feature of lipases is perhaps the key to the great differences in activity and stereoselectivity observed in different reaction media. Furthermore, information about self-association of the lipases in different solvents could be obtained. PSL, but not CVL and ROL, forms aggregates in water. Lipase aggregation can be reversed by the addition of detergent or isopropanol, which competes for the hydrophobic surface domains of this protein. This dissociation could efficiently contribute to the increase in lipase activity in the presence of a detergent or isopropanol.

INTRODUCTION

Lipases belong to the family of lipid-hydrolyzing enzymes (triacylglycerol-acyl hydrolases). They play an important role in intracellular lipid metabolism and extracellular lipid degradation (Woolley and Petersen, 1994). Their wide range of substrate specificities makes them useful as (stereo)selective catalysts in organic chemistry for the (bio) transformation of biologically active compounds or their intermediates (Faber, 1992). In water, the lipophilic substrates of lipases have to be dispersed either by detergent micelles (Ransac et al., 1995) or by the addition of organic solvent. Organic media are preferably used in biocatalysis for selective reactions on synthetic compounds.

The three-dimensional structures of several lipases have already been solved by x-ray crystallography (e.g., Winkler et al., 1990; Noble et al., 1993). Although the amino acid sequences of lipases of different origin are very diverse, they share as a characteristic structural feature the α/β hydrolase fold. Lipases belong to the serine-hydrolase enzymes with the catalytic triad Ser-Asp(Glu)-His. Furthermore, they all have in common a highly conserved consensus sequence G-X-S-X-G around the active site serine. On the other hand, the diversity of lipase amino acid sequences leads to a high structural variability that may account for the large observed functional differences between the different enzymes.

Information on structural properties of lipases in solution, that is under conditions relevant to lipase function, is very scarce. In principle, three-dimensional protein structures in solution at an atomic resolution level can be obtained by NMR spectroscopy. The application of this method is currently limited, however, to a molecular protein mass of 30 kDa in the most favorable case. In addition, much enzyme, typically 10 mg protein/ml, is required. Under such conditions, protein aggregation may occur, which further diminishes data resolution. As we will demonstrate by this work, such problems are already encountered with lipases at submilligram/ml concentrations.

To obtain information on overall structural properties of lipases that may help in the understanding of their physical and functional properties in diluted solution, we initiated a time-resolved fluorescence study on microbial lipases of different origin. The tryptophan residues of these enzymes served as intrinsic fluorescence reporters, providing information on internal molecular mobility, movement of the entire particle, and thus, the degree of protein self-association, as well as the exposure of tryptophans to the solvent, depending on reaction conditions.

We selected three lipases from *Chromobacterium viscosum* (CVL), *Pseudomonas species* (PSL), and *Rhizopus oryzae* (ROL) and studied their structures and functions in different solvent systems. Only the three-dimensional crystal structure of CVL is known (Lang et al., 1996). This enzyme seems to be identical to a lipase from *Pseudomonas*

Received for publication 30 March 1998 and in final form 15 March 1999.
Address reprint requests to Dr. A. Hermetter, Department of Biochemistry, Technische Universität Graz, A-8010 Graz, Austria. Tel.: 43-316-873-6457; Fax: 43-316-873-6952; E-mail: f548herm@mbox.tu-graz.ac.at.

0006-3495/99/07/493/12 $2.00

glumae (Taipa et al., 1995), the crystal structure of which has also been solved (Noble et al., 1993). Fig. 1 *A* shows the backbone structure model of CVL containing three tryptophan residues, which are almost completely buried in the interior of the protein and therefore are hardly accessible to solvent molecules. The structure shown in Fig. 1 *B* is the only projection in which the tryptophans are visible, at least to a minimal extent. From other projections it becomes evident that the respective amino acids are completely buried in the hydrophobic core of the protein. In the case of ROL and PSL, only the amino acid sequences and not the three-dimensional structures have been determined (Haalck, 1994).

We have studied the lipases from CVL, PSL, and ROL in three different solvent systems, because it was known that specific activities and stereoselectivities of these enzymes toward a triacylglycerol-analog substrate were, as a consequence, greatly modified (Zandonella et al., 1995). In contrast to esterases, lipases exhibit maximum activity in the presence of lipid-water interfaces. Lipases are supposed to be much less active in the absence of an activating interface. Crystal structures of lipases with inhibitors bound to the active site (Brzozowski et al., 1991) revealed that the structural difference between a lipase and its complex with an inhibitor is mainly due to the movement of an α-helical segment, or "lid." The catalytic site of the enzyme in its inactive form is covered by the lid, whereas in the active enzyme form, the catalytic triad is exposed because of the movement of the lid. Thus it is supposed that the presence of micelles or organic solvent leads to the same change in protein conformation that activates the enzyme. The extent of activation depends, however, on the "quality" of the interface. To date, conformational changes that are associated with changes in activity have not been reported for lipases in solution. Thus we studied three selected microbial lipases by time-resolved fluorescence spectroscopy to characterize their structures in solutions and to find out how protein conformation and function respond to different solvent conditions.

We found that all three lipases under investigation exhibit very high internal mobility around their tryptophan residues in different solvent systems. Furthermore, it turned out that PSL is aggregated in aqueous buffer. These aggregates dissociate in the presence of detergent micelles or upon addition of organic solvent (isopropanol). CVL and ROL are monomeric in the solvent systems under investigation. Finally, PSL and ROL show different tendencies to change their conformation in the precence of isopropanol, leading to activation or inactivation, depending on the solvent concentration.

MATERIALS AND METHODS

Protein sources and reagents

Commercially available lipases from *Chromobacterium viscosum* (from Toyo Jozo, Japan), *Pseudomonas species* (from Nagase Biochemicals, Japan), and *Rhizopus oryzae* (from Sanofi Chimie, France) were purified to homogeneity (Haalck, 1994).

The lipases were dissolved in 1 M sodium hydrogen phosphate buffer (pH 7.4). The zwitterionic SB12 (sulfobetaine, *N*-dodecyl-*N,N*-dimethyl-ammonio-3-propane-sulfonate from Serva Feinbiochemica GmbH, Germany) was used as a detergent in threefold cmc concentration (10 mM). Isopropanol was from Merck, Germany.

Three-dimensional structural models of CVL were obtained on the basis of data (Lang et al., 1996) retrieved from the NCBI (National Center for Biotechnology Information), using RasWin Molecular Graphics (Windows Version 2.4, ©1993, 1994 R. Sayle).

Fluorescence measurements

Steady-state fluorescence emission spectra and anisotropies were measured with a Shimadzu RF 540 fluorometer. The excitation wavelength was 295 nm. The emission wavelengths varied from 310 nm to 450 nm in 1-nm increments. The slit widths of the excitation and the emission monochromators were set at 10 and 5 nm, respectively.

Anisotropy measurements were carried out with film polarizers from Shimadzu (excitation wavelength: 295 nm, emission wavelength: 330 nm, slit widths: 10 nm for excitation and emission monochromators, respectively). The cuvette holder was thermostatted at 30°C with an external water bath. Anisotropies r were calculated according to

$$r = \frac{I_{VV} - GI_{VH}}{I_W + 2GI_{VH}}$$

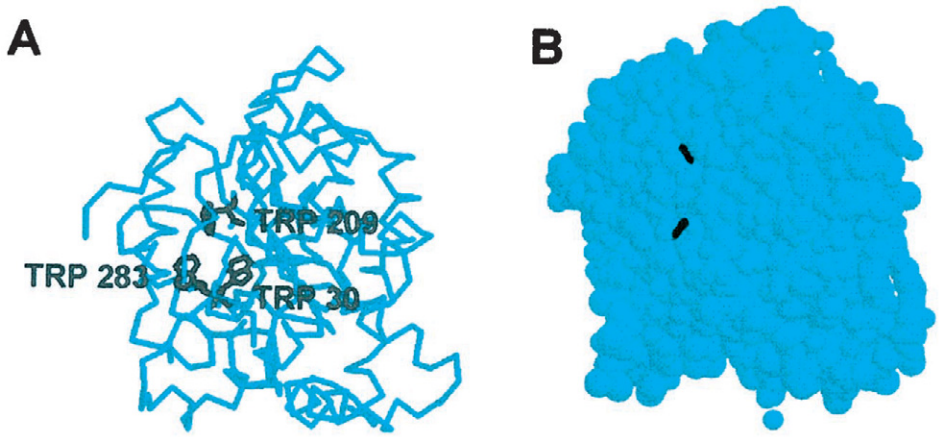

FIGURE 1 Diagram showing the three-dimensional crystal structure of CVL (Lang et al., 1996). (*A*) Backbone structure with the three CVL tryptophan residues (*black sticks*). (*B*) Space-filling model of CVL. CVL tryptophans (*in black*) are completely buried in the interior of the lipase.

where I_{VV} and I_{VH} are, respectively, the intensities parallel and perpendicular to the vertically oriented excitation polarizer. The *G*-factor was determined according to

$$G = I_{HV}/I_{HH}$$

where I_{HV} and I_{HH} are, respectively, the intensities perpendicular and parallel to the horizontally oriented excitation polarizer.

The time-resolved fluorescence measurements were performed using a multifrequency phase and modulation fluorometer. A mode-locked frequency-doubled ND-YAG laser synchronously pumped a cavity-dumped and frequency-doubled rhodamine G6 dye laser (Coherent 700) to obtain an excitation wavelength of 295 nm. The modulation frequencies varied between 10 and 500 MHz. Twenty-five different frequencies were used for one frequency scan. The polarizers, the cuvette holder, and the frequency domain data acquisition equipment were from ISS (Urbana, IL). The fluorescence light was selected by a 335-nm cut-off filter. Neutral density filters (optical density between 0.4 and 1) were used to attenuate the intensity of the laser beam.

For lifetime measurements, the emission polarizer was set at the magic angle of 54.7° relative to the vertically oriented excitation polarizer. The scatter solution LUDOX was used as the reference. The wavelength-dependent fluorescence decay was measured, using interference filters (320, 330, 340, 360, 380, and 400 nm) in the emission light path. For the determination of anisotropy decays, phase angles and demodulations at 25 frequencies between 10 and 500 MHz were measured at parallel and perpendicular orientations of the emission polarizer relative to the vertically oriented excitation polarizer.

Data analysis

Lifetime analysis in terms of exponential decays (Lakowicz et al., 1984) or continuous lifetime distributions (Alcala et al., 1987b) were performed using a program provided by ISS. The standard errors of phase angles and modulations were set at 0.2 and 0.004, respectively. The decay-associated spectra were obtained by combining time-resolved data and steady-state emission spectra. Differential phase angles and the ratios of the polarized modulated amplitudes were used to determine the parameters of the time-dependent anisotropy decay, namely rotational correlation times and their associated amplitudes (Lakowicz et al., 1985). The required computer program (DIFANL) was provided by the Center of Fluorescence (Baltimore, MD). The standard errors of differential phase and modulation values were set at 0.3 and 0.008, respectively. $r(0)$ values have been obtained by fitting of the measured differential phase angles and modulations to the decay models. $r(0)$ has been determined to be 0.27. This value was also used for the transformation of frequency-modulated anisotropy data into the time-resolved anisotropy decay of lipases (Lakowicz, 1983). It is in agreement with $r(0)$ values for protein tryptophans reported in the literature (Sanyal et al., 1987).

Hydrodynamic volumes V_h and Stokes radii r_h of the protein molecules were calculated from the long rotational correlation times, using the Stokes-Einstein equation for the rotation of a rigid sphere:

$$\theta = \frac{\eta MG}{RT}(v + h)$$

where θ is the rotational correlation time of the particle, η is the viscosity of the solvent, *MG* is the molecular mass of the particle, *R* is the gas constant, *T* is the absolute temperature, ν is the specific volume, and *h* is the hydration factor (0.2 ml/mg/0).

Dynamic light scattering

Frozen solutions of lipase from *Rhizopus oryzae* were thawed at 5°C by passing through a 0.02-μm Anatop 25Plus (Merck) filter. The final protein concentration was 0.3 mg/ml. The laboratory-built goniometer was equipped with an Ar^+ laser (Spectra Physics; model 2060-55, P_{max} = 5 W, λ = 514.5 nm), single mode fiber detection, and an ALV-5000 correlator (ALV5000/E, Germany). Measurements were carried out at a scattering angle of 90° at 20°C and a laser power of 1 W. The time dependence of the scattering intensity, represented by its correlation function, provides information on the diffusional motion of the scatterer. Correlation functions from repeated experiments (typically 10 per sample over 5 min) were averaged. The diffusion coefficient *D*, determined from the correlation function, is related to the apparent hydrodynamic radius R_H by the Stokes-Einstein equation, i.e., an equivalent sphere with the radius R_H shows the same diffusion behavior as the particle under investigation and serves as a size parameter. Polydisperse systems give rise to a correlation function with a spectrum of different decay constants. Laplace inversion of the correlation function results in a intensity weighted size distribution $D(R_H)$ (Schnablegger, 1991).

Static light scattering and integrated intensity

The integrated intensity (averaged over long times compared with the time scale of fluctuations in the dynamic experiment) is another, completely independent parameter for the aggregation phenomena. For particles that are small compared to the wavelength of the scattered radiation, this integrated intensity is directly related to the mean mass or aggregation number of the particles and is independent of its diffusion dynamics. Experiments were carried out as described for the dynamic light scattering experiments at 20°C, using a wavelength of 514.5 nm at a 90° scattering angle. Because the particle size is very small compared to the wavelength of the scattered radiation, the scattered intensity measured at 90° can be used as the scattering intensity at $q = 0$, where q is the length of the scattering vector. Pure toluene, which has a Raleigh factor of 23.8E-6 (1/cm) at 20°C and 514.5 nm, was used as a calibration standard. The specific refractive index increment is assumed to be 0.189 ± 0.01 (ml/g). This is a mean value for proteins (Huglin, 1972). With this increment and a protein concentration of 0.3 mg/ml, the molecular mass of the protein was determined (Chu, 1991).

Determination of enzyme activity

The specific activities of lipases were determined with 1(3)-*O*-hexadecyl-2-pyrenedecanoyl-3(1)-trinitrophenylaminododecanoyl-*sn*-glycerols as fluorogenic triacylglycerol-analog substrates. The chemical synthesis and the lipase assay are described elsewhere (Duque et al., 1996; Zandonella et al., 1995). These lipase substrates can be applied to a wide variety of solubilizing media to determine lipase activity. We used mixtures of isopropanol and water at solvent concentrations as indicated in the legends to the figures. The concentration of the substrate was always 2 μM.

Cleavage of the fluorogenic substrates leads to a continuous time-dependent increase in pyrene fluorescence (excitation wavelength: 342 nm, emission wavelength: 378 nm). Typical time scans required 5 min. "Stereoselectivities" were obtained as the ratios of enzyme activities toward the pure enantiomers (1-acyl- versus 3-acyl enantiomer) of the fluorogenic alkyldiacylglycerols as indicated above.

RESULTS

We have studied the physical properties of three different microbial lipases in solution, namely CVL, PSL, and ROL. CVL and PSL show 36% amino acid sequence homology, whereas the sequence of ROL is significantly different. The lipase tryptophans served as intrinsic fluorescence markers for the molecular structure and dynamics of the respective enzymes (Lakowicz, 1983). CVL, PSL, and ROL contain three tryptophans (W-30, W-209, and W-283), two tryptophans (W-28 and W-198), and three tryptophans (W-38, W-46, and W-224), respectively. The three tryptophan res-

idues of CVL are mainly buried within the hydrophobic core of the protein (Fig. 1, *A* and *B*).

Fig. 2 shows the fluorescence emission spectra of CVL, PSL, and ROL in three different solvent systems. Samples were excited at 295 nm to selectively observe the tryptophans and to avoid interference with tyrosine fluorescence. In aqueous buffer, the CVL tryptophans are located in a hydrophobic environment of the protein core (emission maximum at 326 nm). The tryptophans of PSL and ROL are shifted to longer wavelengths, indicating a more polar surrounding for at least one tryptophan (emission maxima at 336 nm and 337 nm, respectively).

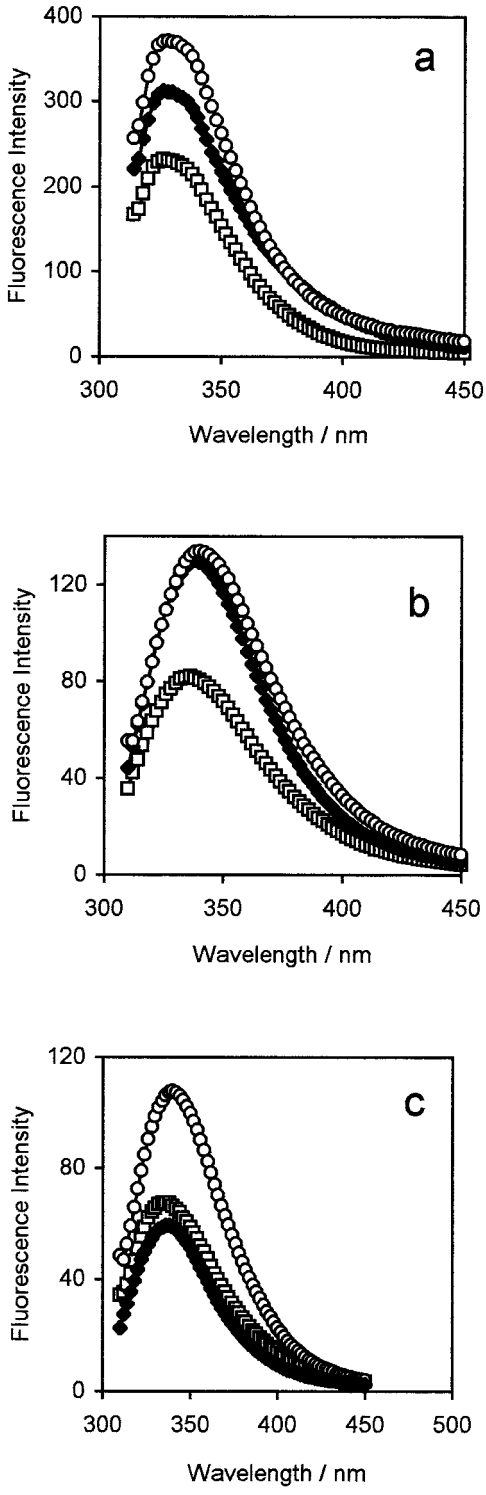

FIGURE 2 Fluorescence emission spectra of protein tryptophans: CVL (*a*), PSL (*b*), or ROL (*c*) in 0.1 M sodium phosphate buffer, pH 7.4 (□), in the presence of SB12 micelles (♦) and in an isopropanol-water mixture (○) (1/1, v/v, for CVL and PSL; 1/4, v/v, for ROL) at 30°C (excitation wavelength 295 nm). Enzyme concentrations were 4 μM.

The emission maxima of tryptophan fluorescence hardly change in the presence of detergent micelles or organic solvent. Therefore the average polarity of the tryptophan surroundings in a given lipase must be the same under these conditions. In contrast, significant changes in fluorescence intensities are observed. The total fluorescence intensity of CVL tryptophans is higher when SB12 micelles (1.3-fold) or isopropanol (1.6-fold) are present. The same effect is found for the tryptophans of PSL. The fluorescence of ROL tryptophans is only increased in the presence of isopropanol (1.3-fold), but not in detergent micelles.

More detailed information about the individual tryptophan environments in the protein molecule is obtained from decay-associated spectra (Fig. 3). Based on the decay times, these spectra have been measured across the emission spectrum (lifetime analysis is described in detail below). Almost the entire fluorescence intensity of CVL tryptophans (Fig. 3 *A*) is due to the decay-associated spectrum of the long-lifetime component emitting at 330 nm, providing evidence that the three tryptophan residues of CVL are located in protein domains of very similar hydrophobicity. The situation is different if we look at the decay-associated spectra of PSL (Fig. 3 *B*), showing three lifetime components. The long and the intermediate ones show the highest fractional intensities. They exhibit the same emission maxima at 340 nm and, thus, the same average environmental polarity, which is higher when compared to CVL. The intensity of the shortest lifetime component is almost negligible.

The decay-associated spectra of the ROL tryptophans reveal that the tryptophan residues of this enzyme must be located in environments of different polarity and/or accessibility to water. The long-living component (λ_{max} at 330 nm) represents a more hydrophobic protein domain compared to the intermediate lifetime component (λ_{max} at 340 nm). The emission maximum of the shortest lifetime component could not be determined (see Fig. 3 *C*).

Lifetimes were determined by the phase and modulation method (Fig. 4). Phase angles and demodulations were measured at 25 different modulation frequencies between 10 and 500 MHz. The data were fitted to various decay models, assuming either exponential decays or continuous lifetime distributions (Table 1 shows the data analysis for CVL).

χ^2_{red} was determined for each decay model as a criterion for the goodness of fit. This parameter was high when single-exponential decays or unimodal lifetimes distributions were used. Adding one more lifetime component resulted in a significantly better fit. A biexponential decay

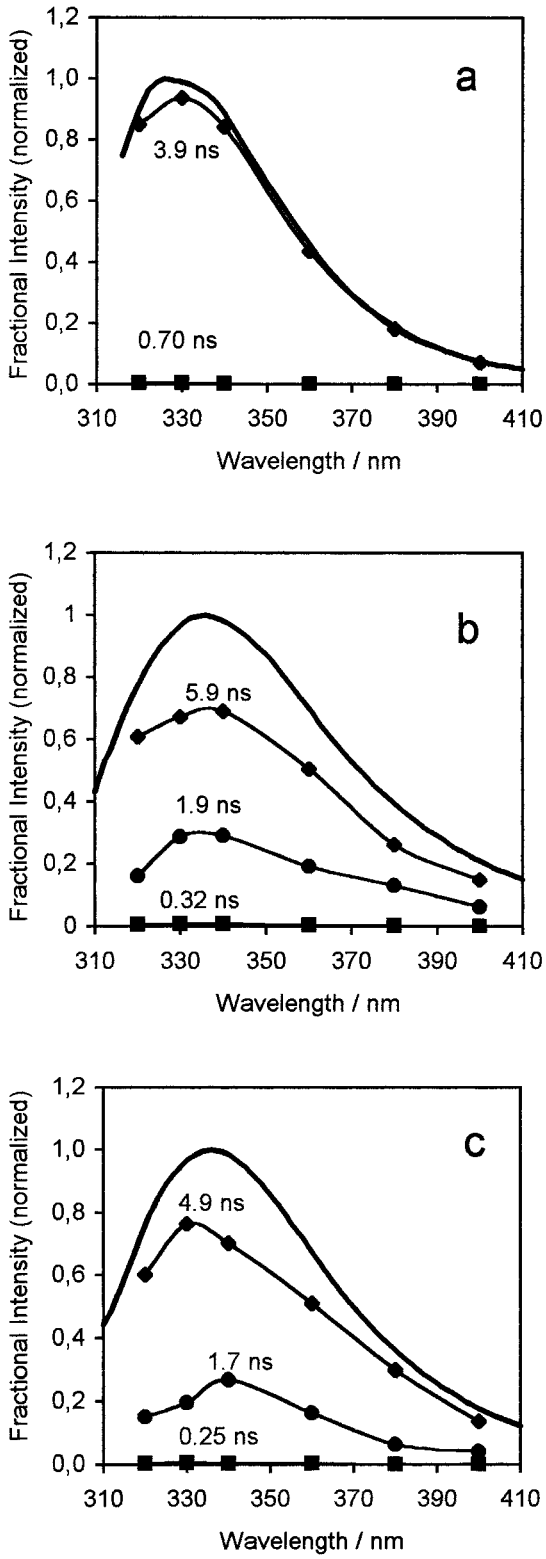

FIGURE 3 Decay-associated spectra of protein tryptophans: CVL (*a*), PSL (*b*), and ROL (*c*) in 0.1 M sodium phosphate buffer, pH 7.4. The lifetime values (τ/ns) indicated in the figures correspond to the lifetime centers of the continuous bimodal (CVL) and trimodal (PSL, ROL) Gaussian lifetime distributions. The steady-state spectra are also shown.

gave a much lower χ^2_{red} as compared to a single-exponential decay or a unimodal lifetime distribution, respectively. χ^2_{red} did not significantly improve on going from a biexponential decay to a bimodal lifetime distribution. Thus, from the statistical point of view, only the biexponential decay model seems to be justified for CVL tryptophan lifetime analysis. However, on a phenomenological basis, it seems to be justified to assume rather a distribution of excited states rather than two discrete states in a dynamical macromolecule (Alcala et al., 1987a,b). Thus we preferred the bimodal lifetime distribution for comparing fluorescence properties of lipases in different solvent systems.

The goodness of fit is not only represented by a comparison of reduced χ^2, but also by the distribution of the residuals of the experimental data in comparison to the calculated data based on a chosen decay model (Fig. 4 shows data for CVL). The unimodal Gaussian distribution shows large and systematic deviations of the residuals. In contrast, an almost perfect fit was obtained for the double-exponential decay or the bimodal lifetime distribution, showing random deviation of measured data from the calculated ones. We are aware of the fact that χ^2_{red} values for the optimal fits are still very high. Apart from inaccuracies in measured phase angles and demodulations, this might be due in part to the chosen decay models, which need not be identical to the parent functions, which are unknown for the multitryptophan proteins under investigation. Furthermore, stability of functional lipases is certainly limited, even at low temperatures. Thus a certain extent of protein denaturation that may give rise to an altered lifetime pattern cannot be excluded under the required experimental conditions.

We analyzed the lifetimes obtained for the lipases in aqueous buffer, in aqueous detergent suspension, and in water-isopropanol mixtures (Fig. 5). The tryptophan fluorescence decay of CVL could be fitted to a continuous bimodal lifetime distribution in all three solvents. In contrast, the fluorescence decays of PSL and ROL tryptophans were fitted to trimodal Gaussian distribution functions (Table 1). The fractions of the second lifetime component of CVL and the third lifetime component of PSL and ROL were almost negligible. Thus CVL tryptophans exhibited basically unimodal Gaussian distribution functions in all three solvent systems, whereas the fluorescence lifetime distributions of PSL and ROL tryptophans were essentially bimodal in these systems.

The influence of an organic solvent (isopropanol) on the bimodal lifetime distributions of ROL and PSL was studied in more detail (Figs. 6 and 7). These enzymes responded very differently to an increase in alcohol concentration. Significant conformational changes of ROL were observed at 20 vol% and 40 vol% isopropanol according to the observed shifts of the lifetime centers and the broadening of the long-lifetime components. These effects are accompanied by an increase in enzyme activity and stereoselectivity. At 20 vol% isopropanol, ROL seems to adopt an "optimal" conformation for its stereoselectivity (sn-1/sn-3 = 97). At an alcohol content of 30 vol%, the activity of ROL still

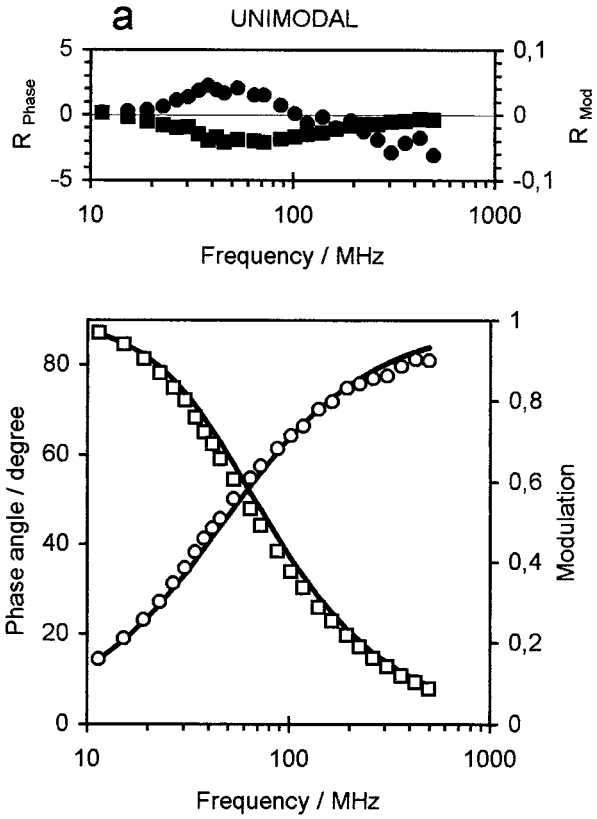

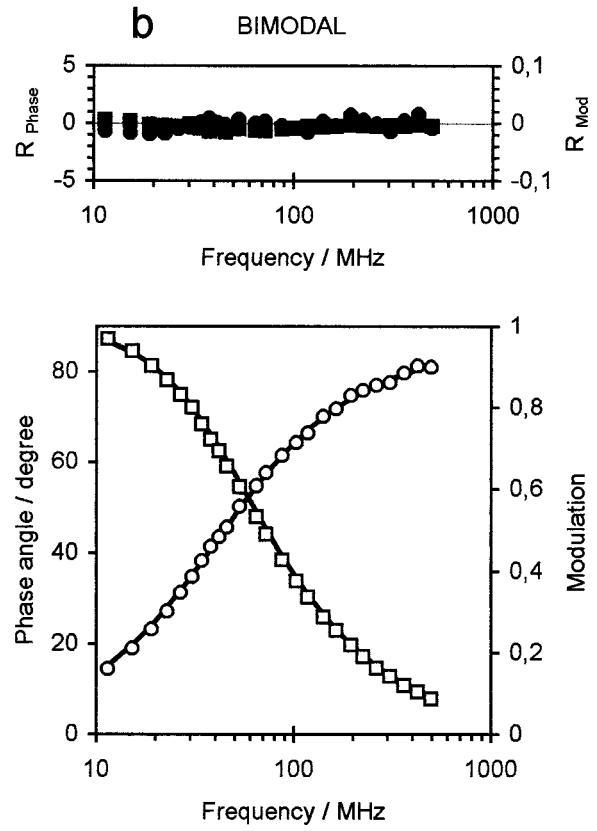

FIGURE 4 Fluorescence decay of CVL tryptophans. Enzyme concentration was 4 μM in 0.1 M sodium phosphate buffer, pH 7.4. Phase angles (○) and modulations (□) measured at different modulation frequencies were fitted to unimodal (*a*) and bimodal (*b*) Gaussian lifetime distributions. In addition, the deviations of measured phase angles (R_{PHASE}, ●) and modulations (R_{MOD}, ■) from the calculated values are shown for the unimodal (*a*) and bimodal (*b*) Gaussian distribution functions.

TABLE 1 Analysis of the fluorescence decay of lipase tryptophans

Enzyme	Fitting-function	τ (ns)	ω (ns)	α	χ^2_{red}
CVL	Exponential				
	Monoexponential	3.57	—	1	74
	Biexponential	3.88	—	0.96	6.7
		0.70	—	0.04	
CVL	Distribution				
	Monomodal	3.57	0.85	1	52
	Bimodal	3.88	0.66	0.97	5.5
		0.70	0.38	0.03	
	Trimodal	3.98	0.13	0.93	5.4
		1.28	0.05	0.065	
		0.00	0.05	0.004	
PSL	Distribution				
	Trimodal	5.91	1.25	0.48	8.4
		1.95	0.37	0.47	
		0.32	0.22	0.05	
ROL	Distribution				
	Trimodal	4.90	0.80	0.53	2.7
		1.68	0.220	0.40	
		0.25	0.07	0.07	

Phase angles and demodulations were determined at 25 different modulation frequencies between 10 and 500 MHz at room temperature, using a 335 nm cut-off filter in the emission light path (excitation wavelength: 295 nm). Data were fitted to the indicated fitting functions (exponentials or continuous Gaussian distributions), assuming errors of phase and modulation of 0.3 and 0.008, respectively. Enzyme concentration was 4 μM in 0.1 M sodium phosphate buffer (pH 7.4).

increases, but stereoselectivity is quite low (sn-1/sn-3 = 4). Above 30 vol% isopropanol in water, the width of the shorter lifetime component is broadened to a large extent, indicating extensive conformational changes of all tryptophan segments. Activity of ROL decreased to a large extent above 30 vol% isopropanol and was totally lost at 50 vol% isopropanol.

In contrast, PSL behaved completely differently (Fig. 7). The lifetime centers of the Gaussian distributions were affected by isopropanol to a lesser extent. There were some small variations in the distribution widths, but neither lifetime distribution broadening nor unfolding could be detected in the presence of 50 vol% alcohol. Enzyme activity even reached its maximum at 50 vol% isopropanol, whereas stereoselectivity remained unchanged. Evidently no critical rearrangement of enzyme conformation and thus no significant changes in the lifetime pattern occurred when this enzyme was subjected to solvents of different alcohol content.

Internal motions and self-association of the lipases were studied by time-resolved fluorescence anisotropies in dif-

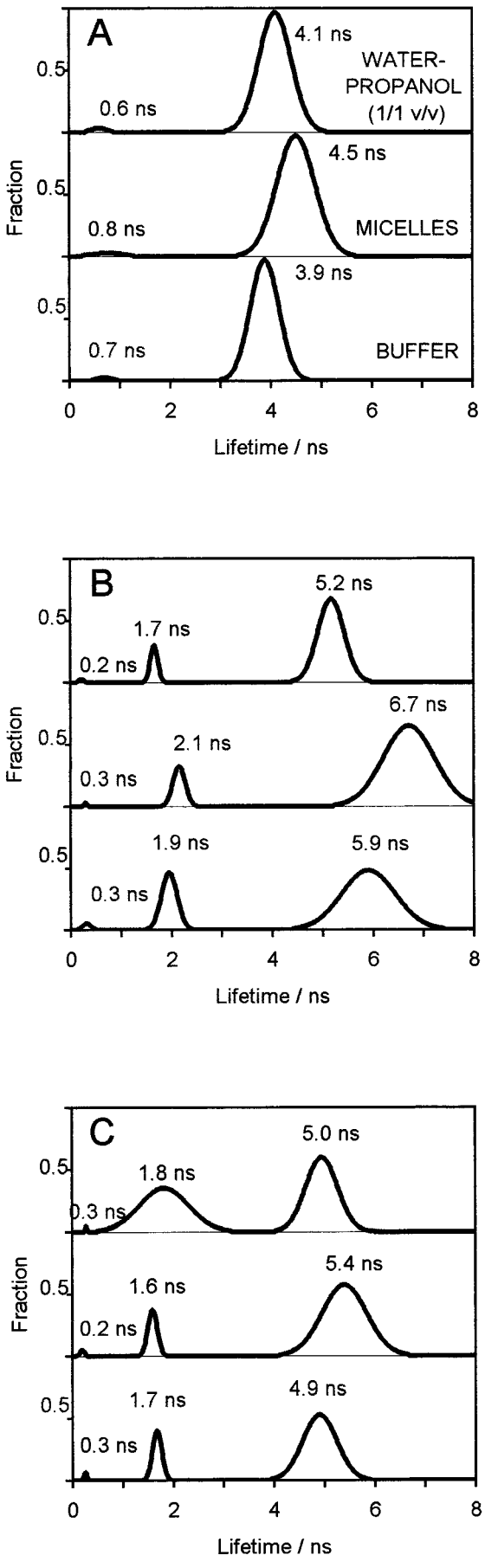

ferent solvents. We measured the differential polarized phase angles and modulations at 25 different frequencies from 10 to 500 MHz (Fig. 8). The frequency-domain data (Fig. 8 *A*) were converted into time domain data by Fourier transform analysis (Fig. 8 *B*). From the time-dependent decay of fluorescence anisotropies of CVL and PSL it can be concluded that the tryptophans of lipases are very mobile, because a large fraction of their anisotropy decays within the first nanosecond. This effect is more pronounced with PSL than with CVL.

Anisotropy data obtained for the lipases in different solvent systems were analyzed in terms of three rotational correlation times (Table 2). No attempt was made to correct for the effect of intramolecular Trp→Trp energy transfer on fluorescence anisotropy (Demchenko, 1992). More than 50% of the anisotropy decay is due to a rotational correlation time in the picosecond range. It is probably associated with the very fast local motions of the fluorophores, contributing significantly to the overall anisotropy decay. The tryptophans of ROL and PSL in particular show very short correlation times, corresponding to the time scale of the motion of free tryptophan in solution. The shortest rotational correlation times for CVL tryptophans were slightly higher as compared to ROL and PSL. The intermediate rotational correlation time is probably due to the movement of larger segments to which the tryptophans are bound. The slowest rotational correlation times of lipase tryptophans reflect the motion of the entire protein molecule, depending on particle size and viscosity of the solvent. From the rotational correlation times, apparent particle sizes could be determined using the Stokes-Einstein equation, taking into account the particular solvent viscosities. The experimental values were compared with particle sizes estimated from the known molecular weights of the lipases under investigation, assuming the same extent of protein hydration (Table 3). We did not compare particle sizes in the presence of SB12-micelles, as we do not know the stoichiometry and type of micelle-lipase interactions. CVL was found to be monomeric in aqueous buffer in the absence and presence of organic solvent. ROL and PSL in aqueous buffer showed hydrodynamic radii that were higher compared to the expected values based on the molecular weights of the respective proteins. In the presence of isopropanol, smaller particle sizes were found, corresponding to the monomeric enzymes. The presence of SB12-micelles leads to a decrease in rotational correlation times, pointing to dissociation of the oligomers, although the extent of this is unknown (data not shown).

FIGURE 5 Fluorescence decay of lipase tryptophans in different solvents. Fluorescence decays were analyzed in terms of bimodal or trimodal Gaussian lifetime distributions: CVL (*A*), PSL (*B*), and ROL (*C*) in 0.1 M sodium phosphate buffer, pH 7.4 (*lower panel*), in the presence of SB12 micelles (*middle panel*), and in an isopropanol-water mixture (1/1, v/v) (*upper panel*) at 30°C (excitation wavelength 295 nm). Indicated are the values of the corresponding lifetime centers. Enzyme concentrations were 4 μM in 0.1 M sodium phosphate buffer, pH 7.4.

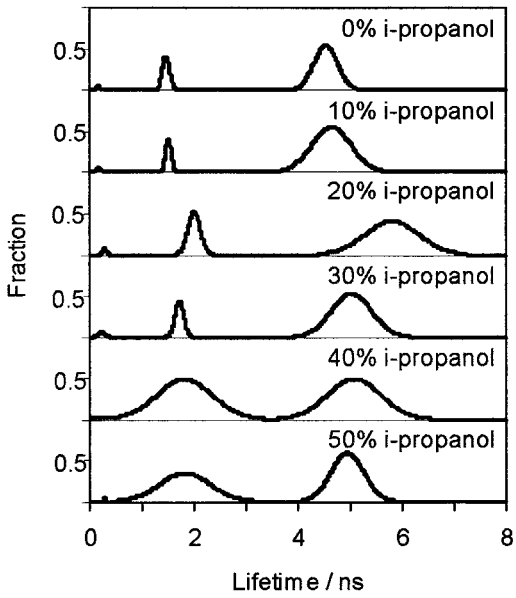

Specific activity (pmol/min/μg)		Stereoselectivity
sn-1	sn-3	sn-1/sn-3
130	6	25
272	4	68
486	5	97
684	175	4
26	14	2
0	0	-

FIGURE 6 Effect of isopropanol on fluorescence lifetimes of ROL tryptophans. Fluorescence decays were analyzed in terms of continuous trimodal Gaussian lifetime distributions. Specific enzyme activities toward the sn-1 and sn-3 acyl enantiomers of fluorogenic alkyldiacylglycerols were determined as described in Materials and Methods. Stereoselectivities are expressed as the ratios of enzyme activities toward the sn-1 and sn-3 acyl enantiomers of the substrate.

The particle size of ROL in aqueous buffer was also determined by light scattering methods. Dynamic light scattering measurements were performed to obtain the hydrodynamic radius of the protein. The result is presented in Fig. 9. The distribution $D(R_H)$ shows a main peak at 3.4 nm and a small peak above 30 nm, which is probably due to the presence of impurities or protein aggregates. It should be emphasized that the number of these large particles is extremely small, taking into account that their contribution to the apparent size distribution scales with R^6. To determine the molecular weight of the protein and thus the degree of protein self-association, we performed, in addition, static light scattering experiments on an absolute scale. The molecular weight of ROL in aqueous buffer was found to be 26.000 $\pm$ 3.400. This value is very close to the theoretical molecular weight of the enzyme. Therefore, we conclude that ROL in aqueous buffer is monomeric.

DISCUSSION

Three microbial lipases, namely CVL, PSL, and ROL, have been studied by steady-state and time-resolved fluorescence spectroscopy to obtain information on the biophysical properties of these enzymes under native conditions in solution. The "solvents" employed were aqueous buffer, detergent micelles (SB12), or alcohol-water mixtures (isopropanol-water). Such additives are usually required for solubilization of the water-insoluble substrates (triacylglycerols) of lipases.

Protein tryptophans, which are sensitive to polar and apolar interactions with their environment, served as spectral probes. When tryptophans are transferred from an aqueous to a lipid phase, a blue shift of the emission maximum and an increase in fluorescence intensity can be observed (Lakowicz, 1983). In agreement with the three-dimensional structure of CVL (Lang et al., 1996), the emission spectra of CVL tryptophans are blue-shifted, indicating that these residues are located in the hydrophobic interior of the protein. The CVL emission maximum remains unchanged in the presence of a detergent or isopropanol, providing evidence that the fluorophores are still well shielded from the solvent under these conditions. These data are in agreement with lifetime distributions, which were also found to be very similar in these reaction systems. From the decay-associated emission spectra it can be inferred that CVL tryptophans are located in protein regions of similar polarity.

PSL exhibits a 36% sequence homology to CVL and carries only two tryptophan residues. Compared with CVL, fluorescence emission maxima of PSL are red-shifted in the solubilization systems under investigation. A more "polar" fluorescence (λ_{max} red-shifted as compared to CVL) was also observed for the three ROL tryptophans. From the decay-associated emission spectra of ROL it can be inferred that its tryptophans are probably located in protein environ-

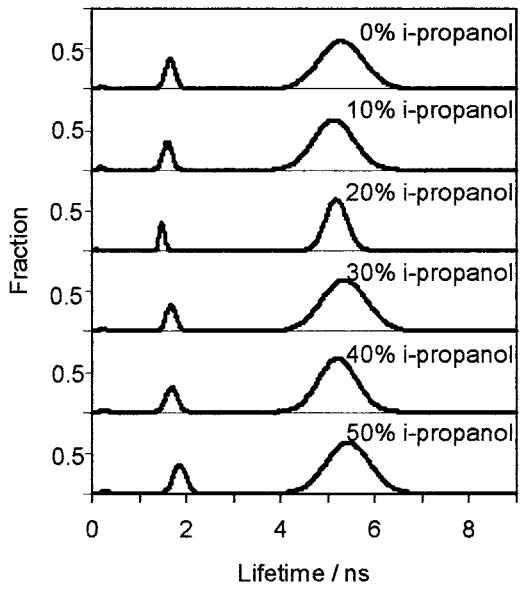

	Specific activity pmol/min/μg		Stereoselectivity
	sn-1	sn-3	sn-1/sn-3
0% i-propanol	22	53	0.4
10% i-propanol	38	75	0.5
20% i-propanol	117	111	1.0
30% i-propanol	263	172	0.7
40% i-propanol	774	609	1.5
50% i-propanol	982	2008	0.5

FIGURE 7 Effect of isopropanol on fluorescence lifetimes of PSL tryptophans. Fluorescence decays were analyzed in terms of trimodal Gaussian lifetime distributions. Specific enzyme activities toward the sn-1 and sn-3 acyl enantiomers of fluorogenic alkyldiacylglycerols were determined as described in Materials and Methods. Stereoselectivities are expressed as the ratios of enzyme activities toward the sn-1 and sn-3 acyl enantiomers of the substrate.

ments of different hydrophobicity. Except for ROL in micelles, fluorescence intensity increased in the presence of a detergent or isopropanol. This effect can be due to change in protein conformation as well as the degree of protein self-association. We did not find any consistent correlation between intensity and lifetime in any of the solvent systems we used. Such interrelationships might be obscured in multitryptophan proteins, because amino acids in different proteins may respond to "solvent" effects (polarity, aggregation) to a different extent.

The fluorescence lifetime distributions were determined to obtain information about conformational changes in different solvents. Our interpretation of the tryptophanyl fluorescence decay in terms of lifetime distributions is based on the assumption that lifetime heterogeneity arises from the multitude of different conformational states and substates that a protein may assume as a consequence of structural fluctuations (Alcala et al., 1987a; Bismuto et al., 1989). The fluorescence decay of CVL tryptophans could essentially be fitted to a unimodal Gaussian distribution function, whereas ROL and PSL tryptophans essentially exhibited bimodal Gaussian distributions. The addition of a second lifetime component in the case of CVL and the addition of a third lifetime component in the case of PSL or ROL fluorescence decay improved the fit significantly, but the respective fractions were negligible. In the bimodal lifetime distribution model (PSL and ROL), the long-lifetime component may originate from conformations with little interaction with the environment, whereas the shorter lifetimes are probably the result of dynamic quenching by the solvent or the protein matrix (Vos et al., 1995). More specifically, the shorter lifetime component of ROL and PSL might be due to interactions of the surface-exposed tryptophans with the solvent. According to their emission spectra (Fig. 2), these fluorophores are located in more hydrophilic environments of the lipase molecules compared to the CVL tryptophans, which are totally buried in the hydrophobic protein core. The latter tryptophans are not in contact with the solvent and as a consequence show an almost unimodal fluorescence decay. A monoexponential decay for tryptophans can only be expected in a very hydrophobic environment with restricted mobility (Ludescher et al., 1985). One lifetime is probably not enough to account for the decay of a fluctuating single-tryptophan protein. Actually, it has been shown that decays of single-tryptophan proteins are biexponential (Pokalsky et al., 1995). The time-dependent environment of the tryptophan residues in a protein matrix and their interactions with the solvent may give rise to additional heterogeneity of tryptophanyl fluorescence decays. Therefore, we did not apply exponential functions to the lifetime analysis of lipase tryptophans. Heterogeneity of tryptophan lifetimes is probably better described by a distribution of lifetimes (Alcala et al., 1987a).

The structure of CVL seems to be very stable, because there are only minimal variations in the lifetime distributions of the tryptophans with the addition of isopropanol. CVL is enzymatically active in all solvent systems under investigation. In contrast, ROL and PSL show more con-

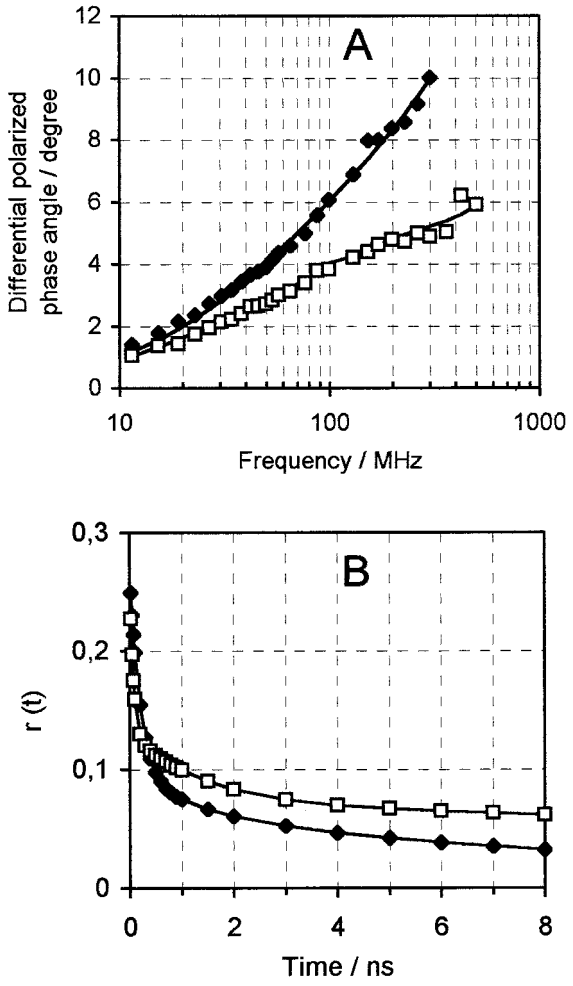

FIGURE 8 Time-resolved fluorescence anisotropy decay of lipase tryptophans. (*A*) Differential polarized phase angles as a function of modulation frequencies for CVL (♦) and PSL (□) in 0.1 M sodium phosphate buffer (pH 7.4) at room temperature. Enzyme concentration was 4 μM. (*B*) Time-dependent fluorescence anisotropy decay $r(t)$ obtained by Fourier transform of experimental frequency domain data for CVL (♦) and PSL (□).

formational flexibility, depending on the solvent, compared to CVL. Lifetime distributions are much more affected by organic solvent in the case of ROL and PSL, whereas CVL lifetimes are hardly affected (Fig. 5). CVL seems to be very stable, even in 50% isopropanol-water mixtures, and shows its highest activity under these conditions (Zandonella et al., 1995), presumably as a consequence of solvent effects on protein conformation and substrate presentation.

To obtain more information about the effect of isopropanol on lipase structures, we compared changes in lipase activities with changes in the observed biophysical properties (lifetime distributions) of ROL and PSL. ROL lifetime distributions were highly affected by the addition of isopropanol. An intermediate broadening of lifetime distributions was induced in the concentration range between 20 vol% and 30 vol% alcohol, probably as a consequence of higher protein mobility. This effect is associated with a dramatic

TABLE 2 Rotational correlation times [θ] of tryptophan residues of CVL, PSL, and ROL in different solvents

Enzyme	Solvent	θ_1/ns (g_1)	θ_2/ns (g_2)	θ_3/ns (g_3)	χ^2_{red}
CVL	Buffer	0.20 (0.64)	1.3 (0.13)	12 (0.23)	3.1
	SB12 micelles	0.06 (0.46)	0.6 (0.23)	14 (0.31)	1.8
	Isopropanol-water (1/1 v/v)	0.26 (0.56)	3.3 (0.14)	33 (0.30)	3.4
PSL	Buffer	0.07 (0.52)	1.5 (0.22)	62 (0.26)	1.8
	SB12 micelles	0.08 (0.53)	2.0 (0.22)	33 (0.25)	9.6
	Isopropanol-water (1/1 v/v)	0.10 (0.57)	2.2 (0.20)	19 (0.23)	10.1
ROL	Buffer	0.06 (0.46)	1.8 (0.17)	32 (0.37)	1.2
	SB12 micelles	0.05 (0.48)	2.2 (0.24)	26 (0.28)	4.5
	Isopropanol-water (1/4 v/v)	0.05 (0.42)	1.1 (0.13)	16 (0.45)	1.9

Differential phase angles were determined at 25 different modulation frequencies between 10 and 500 MHz and fitted to a triple exponential anisotropy decay (best fit according to minimization of reduced chi-square (χ^2_{red}) (see Materials and Methods). Indicated are rotational correlation times θ_i and the respective fractions g_i. r_0 was 0.27. Errors of measured rotational correlation times were between ±10% and ±30%. Enzyme solutions contained 4 μM protein in 0.1 M sodium phosphate buffer, pH 7.4.

change in enzyme activity and stereoselectivity, demonstrating that there is a delicate balance between gain and loss of enzyme function in a two-component reaction system, depending on individual solvent concentrations. Only when large amounts of organic solvents (40–50 vol% isopropanol) are added does ROL become inactivated. This inactivation is accompanied by a dramatic broadening of lifetime distributions. This effect is probably not the result of extensive protein unfolding, because the steady-state spectra of ROL tryptophans are not red shifted. Thus the protein structure must still be compact to prevent the fluorophores from being exposed to water. Despite the lack of

TABLE 3 Comparison of experimental (θ_{exp}) and calculated (θ_{calc}) rotational correlation times and Stokes radii (r_{exp} and r_{calc})

		Experimental			Calculated		
Enzyme	System	θ_{exp} (ns)	$V_{h\ exp}$ (ml/mol)	r_{exp} (Å)	θ_{calc} (ns)	$V_{h\ calc}$ (ml/mol)	r_{calc} (Å)
CVL	Buffer	12	36540	24	15	38400	25
	Propanol-water (1/1 v/v)	33	48720	27	29	42240	26
PSL	Buffer	62	151032	39	15	36000	24
	Propanol-water (1/1 v/v)	19	28050	22	27	39600	25
ROL	Buffer	32	77952	31	15	36000	24
	Propanol-water (1/4 v/v)	16	29416	23	34	37710	25

Experimental rotational correlation times were obtained as indicated in Table 2. Rotational correlation times for an isotropic particle corresponding to the molecular weight of lipases were calculated using the Stokes-Einstein equation (see Materials and Methods). V_h = hydrodynamic volume of a sphere.

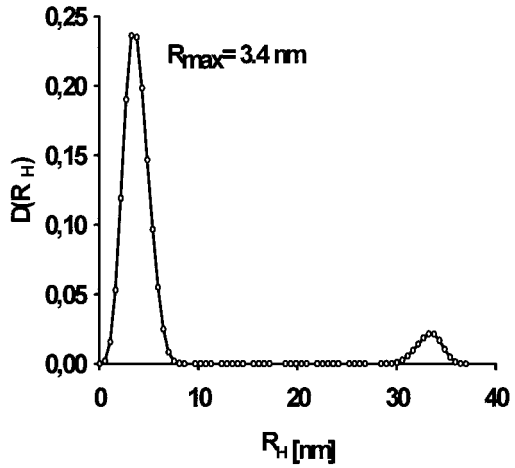

FIGURE 9 Hydrodynamic radius of ROL in aqueous buffer as determined by dynamic light scattering. Shown is the size distribution resulting from a Laplace inversion of the time correlation function. The intensity distribution plotted as a function of the hydrodynamic radius R_H shows a main peak located at 3.4 nm and a small side peak above 30 nm, which can probably be attributed to the hydrated enzyme (main peak) and larger protein aggregates/or impurities (side peak).

significant unfolding, ROL is inactivated in the presence of 50% isopropanol. This is a rather unusual observation. It could be a peculiarity of an interfacially active enzyme whose function is significantly modulated by interaction with apolar molecules that help to maintain rather than destroy their three-dimensional structures (Ransac et al., 1995).

Such inactivation in 50% isopropanol-water mixtures was not observed with PSL. Its lifetime distributions all look the same at different isopropanol concentrations. In addition, stereoselectivity is hardly influenced by the addition of isopropanol. However, PSL activity is highly stimulated by increased alcohol concentrations. This effect might again be due to an altered enzyme conformation as well as a more effective substrate presentation to the enzyme (smaller particle size, increased fluidity, and thus, availability of the substrate in the lipid particle). Furthermore, PSL aggregates in water, and these aggregates dissociate in the presence of isopropanol, generating monomers that might be more active than the protein complexes.

In an attempt to interpret structure-activity relationships for enzymes in water containing organic solvent, we have to take into account that activity of lipases is pH-dependent. However, we did not determine the effect of pH on the fluorescence properties of the lipases. This will be the subject of further investigation.

According to the time-resolved anisotropy data presented in this study, lipases exhibit very high internal mobility of their tryptophan residues compared to other proteins (for a comparison see Steiner, 1983). This is perhaps a peculiar feature of lipases and the key to their great diversity of functional properties, such as activity and stereoselectivity in different reaction media. Using a monolayer study on lipoprotein lipase, Verger (1997) has already demonstrated that lipases may undergo considerable conformational changes, depending on external forces (lateral pressure), which in turn are associated with alterations in functional properties (activity and stereoselectivity).

Time-resolved anisotropies provided information about hydrodynamic particle size of the lipases in different solvents, depending on the extent of protein hydration and self-association. CVL seems to be monomeric in aqueous solution. Assuming the same extent of protein hydration, the hydrodynamic radius of ROL in aqueous buffer would be in support of a protein dimer (r_{exp} = 3.1 nm; see Table 3). This was confirmed by dynamic light scattering experiments leading to a similar value (r_{exp} = 3.4 nm; see Fig. 9). However, a molecular mass of 26 kDa was obtained from static light scattering measurements, indicating the presence of a protein monomer. Thus the apparently larger hydrodynamic size of ROL is not likely to be a consequence of protein association. Rather, it might be a consequence of efficient particle hydration because, according to the known x-ray structures of other (homologous) lipases, deviation from globular shape probably does not account for this result. In contrast, the hydrodynamic particle size of PSL is too large to be indicative of an extensively hydrated protein monomer and probably reflects protein aggregation to a significant extent. This observation is in line with the known x-ray structures of lipases, showing that large domains of the surface of these enzymes are hydrophobic (Brzozowski, 1991), thus favoring protein self-association in aqueous buffer. PSL aggregation was reversed by the addition of detergent or isopropanol competing for the hydrophobic surface domains of the protein. This protein dissociation could effectively contribute to the observed increase in lipase activity in the presence of detergent or isopropanol.

We are indebted to H. Malak for invaluable practical advice.

Financial support by the Austrian Science Foundation (FWF, projects F0107 to A.H. and P 12611-CH to O.G.) is gratefully acknowledged. The experimental work was carried out in part at the Center for Fluorescence Spectroscopy of the University of Maryland at Baltimore (director: Prof. J. R. Lakowicz).

REFERENCES

Alcala, J., E. Gratton, and F. Prendergast. 1987a. Fluorescence lifetime distributions in proteins. *Biophys. J.* 51:597–604.

Alcala, J., E. Gratton, and F. G. Prendergast. 1987b. Interpretation of fluorescence decays in proteins using continuous lifetime distributions. *Biophys. J.* 51:925–936.

Bismuto, E., G. Irace, and E. Gratton. 1989. Multiple conformational states in myoglobin revealed by frequency domain fluorometry. *Biochemistry.* 28:1508–1512.

Brzozowski, A., U. Derewenda, Z. Derewenda, G. Dodson, D. Lawson, J. Turkenburg, F. Bjorkling, B. Huge-Jensen, S. Patkar, and L. Thim. 1991. A model for interfacial activation in lipases from the structure of a fungal lipase-inhibitor complex. *Nature.* 351:491–494.

Chu, B. 1991. Laser Light Scattering: Basic Principles and Practice. Academic Press, San Diego.

Demchenko, A. P. 1992. Fluorescence and dynamics in proteins. *In* Topics in Fluorescence Spectroscopy, Vol. 3, Biochemical Applications. J. R. Lakowicz, editor. Plenum Press, New York and London. 81–83.

Duque, M., M. Graupner, H. Stütz, I. Wichert, R. Zechner, F. Paltauf, and A. Hermetter. 1996. New fluorogenic triacylglycerol analogs as substrates for the determination and chiral discrimination of lipase activities. *J. Lipid Res.* 37:868–876.

Faber, K. 1992. Biotransformations in Organic Chemistry. Springer Verlag, Berlin and Heidelberg.

Haalck, L. 1994. Reinigung und Charakterisierung der mikrobiellen Lipasen aus *Chromobacterium viscosum*, *Pseudomonas sp*. und *Rhizopus arrhizus.* Dissertation. Westfälische-Wilhelms-Universität, Münster, Germany.

Lakowicz, J. R. 1983. Principles of Fluorescence Spectroscopy. Plenum Press, New York and London.

Lakowicz, J. R., G. Laczko, H. Cherek, M. Limkeman, and E. Gratton. 1984. Analysis of fluorescence decay kinetics from variable-frequency phase shift and modulation data. *Biophys. J.* 46:463–477.

Lakowicz, J. R., G. Laczko, I. Gryczynski, and H. Cherek. 1985. Time-resolved fluorescence anisotropies of fluorophores in solvents and lipid bilayers obtained from frequency-domain phase-modulation fluorometry. *Biochemistry.* 24:376–383.

Lang, D., B. Hofmann, L. Haalck, H. J. Hecht, F. Spener, R. D. Schmid, and D. Schomburg. 1996. Crystal structure of a bacterial lipase from *Chromobacterium viscosum* ATCC 6918 refined at 1.6 Ångstroms resolution. *J. Mol. Biol.* 259:704–717.

Ludescher, R., J. Volwerk, G. de Haas, and B. Hudson. 1985. Complex photophysics of the single tryptophan of porcine pancreatic phospholipase A_2, its zymogen, and an enzyme/micelle complex. *Biochemistry.* 24:7240–7249.

Noble, M. E. M., A. Cleasby, L. Johnson, M. Egmond, and L. Frenken. 1993. The crystal structure of triacylglycerol lipase from *Pseudomonas glumae* reveals a partially redundant catalytic aspartate. *FEBS Lett.* 331:123–128.

Noble, M., A. Cleasby, L. N. Johnson, M. R. Egmond, and L. G. Frenken. 1994. Analysis of the structure of *Pseudomonas glumae* lipase. *Protein Eng.* 7:559–562.

Pokalsky, C., P. Wick, E. Harms, F. Lyle, and R. Van Eton. 1995. Fluorescence resolution of the intrinsic tryptophan residues of bovine protein tyrosyl phosphatase. *J. Biol. Chem.* 270:3809–3815.

Ransac, S., F. Carriere, E. Rogalska, R. Verger, F. Marguet, G. Buono, E. Pinho Melo, J. M. S. Cabral, M.-P. Egloff, H. van Tilbeurgh, and C. Cambillau. 1995. The kinetics, specificities and structural features of lipases. Proceedings of the NATO-ASI workshop on "Engineering of/with Lipases" (Porto).

Sanyal, G., M. Charlesworth, R. Ryan, and F. G. Prendergast. 1987. Tryptophan fluorescence studies of subunit interaction and rotational dynamics of human luteinizing hormone. *Biochemistry.* 26:1860–1866.

Schnablegger, H., and O. Glatter. 1991. Optical sizing of small colloidal particles: an optimized regularization technique. *Appl. Optics.* 30:4889–4896.

Steiner, R. 1983. The use of fluorescence anisotropy decay in the study of biological macromolecules. *In* Excited States of Biopolymers. Plenum Press, New York. 154–157.

Taipa, M. A., K. Liebeton, J. V. Costa, J. M. Cabral, and K. E. Jaeger. 1995. Lipase from *Chromobacterium viscosum*: biochemical characterization indicating homology to the lipase from *Pseudomonas glumae*. *Biochim. Biophys. Acta.* 1256:396–402.

Verger, R. 1997. "Interfacial activation" of lipases: facts and artifacts. *Trends Biotechnol.* 15:32–38.

Vos, R., Y. Engelborghs, J. Izard, and D. Baty. 1995. Fluorescence study of the three tryptophan residues of the pore-forming domain of colicin A using multifrequency phase fluorometry. *Biochemistry.* 34:1734–1743.

Winkler, F. K., A. D'Arcy, and W. Hunziker. 1990. Structure of human pancreatic lipase. *Nature.* 343:767–770.

Woolley, P., and S. Petersen. 1994. Lipases: Their Structure, Biochemistry and Application. Cambridge University Press, Cambridge.

Zandonella, G., L. Haalck, F. Spener, K. Faber, F. Paltauf, and A. Hermetter. 1995. Inversion of lipase stereospecificity for fluorogenic alkyldiacyl glycerols. Effect of substrate solubilization. *Eur. J. Biochem.* 231:50–55.